A Digital System for Surface Reconstruction

Weiyang Zhou, Robert H. Brock, and Paul F. Hopkins

Abstract

A digital photogrammetric system, STEREO, was developed to determine three-dimensional coordinates of points of interest (POIs) defined with a grid on a textureless and smooth-surfaced specimen. Two CCD cameras were set up with unknown orientation and recorded digital images of a reference model and a specimen. Points on the model were selected as control or check points for calibrating or assessing the system. A new algorithm for line feature detection called local maximum convolution (LMC) helped extract the POIs from the stereo image pairs. The system then matched the extracted POIs and used a least-squares "bundle" adjustment procedure to solve for the camera orientation parameters and the coordinates of the POIs. An experiment with STEREO found that the standard deviation of the residuals at the check points was approximately 24 percent, 49 percent, and 56 percent of the pixel size in the X, Y, and Z directions, respectively. The average of the absolute values of the residuals at the check points was approximately 19 percent, 36 percent, and 49 percent of the pixel size in the X, Y, and Z directions, respectively. With the graphical user interface, STEREO demonstrated a high degree of automation, and its operation does not require special knowledge of photogrammetry, computers, or image processing.

Introduction

To meet the needs of mechanics experiments, a linear image strain analysis (LISA) system was developed (Choi *et al.*, 1991). This system measures the deformation of a specimen in two dimensions with high accuracy. Many experiments have been carried out with this system on various paper specimens. But, with LISA, the deformation of the specimen in the out-of-plane direction cannot be measured. A project started in 1991 to develop a system for reconstructing surfaces in three dimensions. Zhou *et al.* (1992) reported on the early results of this project. Since then, the system, now called STEREO, has been changed and improved substantially. This paper outlines the implementation of STEREO and the results of experiments with this system.

STEREO has to meet several requirements imposed by mechanical experiments. First, the system needs to satisfy many experimental conditions and yield results speedily with little operator intervention. This requirement excludes the use of traditional photogrammetry, which often requires excessive time combined with particular skills and equipment. Second, the system should be accurate relative to its hardware limitations. The sensitive recording part of a CCD (charge coupled device) camera is a chip with an array of micro-sensors, each corresponding to a pixel in the output image. S_L and S_W, a CCD camera's ability to measure coordinates in the image plane in the length and width directions, respectively, can be calculated:

$$S_L = \frac{L}{N_L} = \frac{8.8}{560} \approx 0.0157 \ (mm/sensor) \quad (1)$$

$$S_W = \frac{W}{N_W} = \frac{6.6}{482} \approx 0.0137 \ (mm/sensor) \quad (2)$$

where W and L are the width and length of the CCD chip, respectively, and N_W and N_L are the number of micro sensors in the width direction and length direction, respectively. With the Panasonic WV-CD20 CCD cameras used in this experiment, $N_W = 482$ and $N_L = 560$, and W and L are specified in the manual to be 6.6 mm and 8.8 mm, respectively. The above equations show that the values S_L and S_W are larger than the actual ability to measure coordinates on a film or a diapositive, which is typically ± 0.005 mm. The accuracy of the system is assessed in terms of pixel sizes, i.e., the average area a pixel covers on the surface of the object being observed.

The field of photogrammetry is shifting from traditional film-based technologies to digital image-based ones. This new trend, called digital photogrammetry or softcopy photogrammetry, is a field that is closely related to the vision technologies with the common ultimate goal of three-dimensional (3D) perception (Wong, 1992). Because it is an emerging field, an exact definition for softcopy photogrammetry or a softcopy photogrammetric workstation is still evolving. However, it is widely accepted that a softcopy photogrammetric workstation includes image processing, three-dimensional coordinate calculation and other functionalities, and operates interactively and automatically toward the completion of photogrammetric tasks (Dowman *et al.*, 1992; Schenk and Toth, 1991). In this sense, STEREO is a highly automated softcopy photogrammetric workstation which works exclusively with digital images of surfaces that need artificial texture. The objective of this paper is to summarize the design and implementation of STEREO and assess its speed, accuracy/precision, and degree of automation.

Implementation and Overview of the System

Surface reconstruction using digital photogrammetry includes four major steps: image acquisition, image processing/matching, coordinate calculation, and interpolation/visual presentation. STEREO contains the functionalities for the first three steps, and the last step was accomplished with functions from the SAS (Statistical Analysis System) and ARC/INFO packages available on other computers at Syracuse University and the State University of New York, College of Environmental Science and Forestry.

In order to calibrate and assess the system, a reference model is used to define points with known spatial positions as either control or check points. Image acquisition includes setting up the hardware (including the model), defining points of interest with a grid on the surface of the specimen

College of Environmental Sciences and Forestry, State University of New York, 1 Forest Drive, Syracuse, NY 13210. W. Zhou is presently with the Science Department, Hughes STX Corporation, EROS Data Center, Sioux Falls, SD 57198.

Photogrammetric Engineering & Remote Sensing, Vol. 62, No. 6, June 1996, pp. 719–726.

0099-1112/96/6206–719$3.00/0
© 1996 American Society for Photogrammetry and Remote Sensing

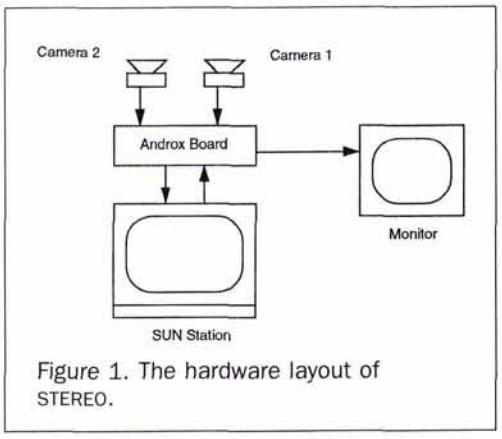

Figure 1. The hardware layout of STEREO.

to be observed, and taking images of the model and the specimen. The cameras need to be set up and kept undisturbed during the period of image acquisition. Additional details about the reference model will be given later while describing the experiment.

Image processing/matching is the key part of the reconstruction procedure. It contains the following steps: detecting the features present in each image (feature detection), determining the sub-pixel-precision location of the features in each image (feature positioning), and, finally, matching corresponding features in the images from a stereo pair (image matching). Coordinate calculation is then achieved with a single process of least-squares adjustment. The steps of image processing/matching and coordinate calculation are described more fully later in this paper.

Figure 1 shows the hardware of this system, consisting of the components listed below:

- The host computer, a SUN SPARC station 330 with 16-Mbyte memory and a 1/4-inch tape drive;
- Androx ICS-400 image processing system with a total of 3 Mbytes of memory and an extensive library of graphics and image processing routines that can be called by C programs; and
- Two Panasonic WV-CD20 CCD cameras with a resolution of 560 by 482 pixels and a set of changeable lenses.

The software package for this system is designed and programmed using object oriented techniques. The whole package consists of approximately 13,000 lines of C code with three basic components: a graphical user interface, image handling (including acquisition, processing, and matching), and coordinate calculation. Each of these components contains many objects, or single-purpose routines, which are implemented independently either by building an interface to the Androx library or by writing a piece of full-length site-specific code. The single-purpose routines for image processing or for photogrammetric operations can be executed individually through the graphical user interface of STEREO. They can also be combined into sequences to form fixed procedures for achieving the functionalities of the basic components of STEREO or their sub-units. The fixed procedures can also be initiated by clicking the corresponding buttons in the graphical interface of STEREO. An operator can go from image acquisition to result output by following the instructions shown in pop-up windows, making a few choices, and answering several questions. Because of the way STEREO is designed and implemented, a fixed procedure can be modified with little change in the code by replacing some objects in its sequence with some others. A new fixed procedure can be defined for a certain objective through experiments by optimizing the combination of single-purpose routines. From this standpoint, STEREO is also an experimental platform for researching new methods of surface reconstruction. Figure 2 summarizes the software structure of the system.

Image Processing/Matching

The general problem of automatically matching stereo image pairs to yield three-dimensional coordinates continues to be researched (Dowman *et al.*, 1992). Prior to image matching, most methods require that the relative orientation of the cameras be known (Grimson, 1981, Grimson, 1985; Keating *et al.*, 1975; Wong and Ho, 1986), or that the stereopair is somehow oriented (Mason and Wong, 1992; Schenk *et al.*, 1992). However, in the special case of this project, despite the fact that the camera orientations are unknown, a few factors make automatic matching less difficult. The observed surfaces are geometrically continuous and the images from the CCD cameras are noise-free relative to aerial photos or satellite images. The most important factor is the freedom to create texture on the surfaces, which are usually blank sheets of paper. With STEREO, points on the surface of the specimen are defined by a grid, which may be drawn with a pen or projected with a slide projector. The grid does not have to be regular or well-defined.

For this project, in order to extract the line features in the image and match the stereo pair automatically, a very efficient and effective algorithm called local maximum convolution (LMC) was developed by Zhou. An LMC is accomplished using a 1 by N ($N = 2n + 1$, $n = 1, 2, 3, \ldots$) template oriented in the column or row direction of an image. The output image from an LMC has the same dimension as the original image and contains only $N + 1$ grey values (0, 1, 2, ..., N). Line features in the original image are usually highlighted by pixels with the value of N in the output image. Suppose the original image has C columns and R rows, numbered from 1 to C and from 1 to R, respectively. Let $max(x, y)$ and $min(x, y)$ denote the greater and smaller one of two integers x and y, respectively. If $p(i, j)$ and $q(i, j)$ are the grey values of a pixel at the ith column and the jth row in the input and output image of an LMC, respectively, then

$$q(i,j) = \sum_{k=max(1,i-N+1)}^{i} u\left(\sum_{l=k}^{min(C,k+N-1)} [u(p(i,j) - p(l,j))] - N \right)$$

when the template is in the horizontal direction (the row direction); and

$$q(i,j) = \sum_{k=max(1,j-N+1)}^{j} u\left(\sum_{l=k}^{min(R,k+N-1)} [u(p(i,j) - p(i,l))] - N \right)$$

when the template is in the vertical direction (the column di-

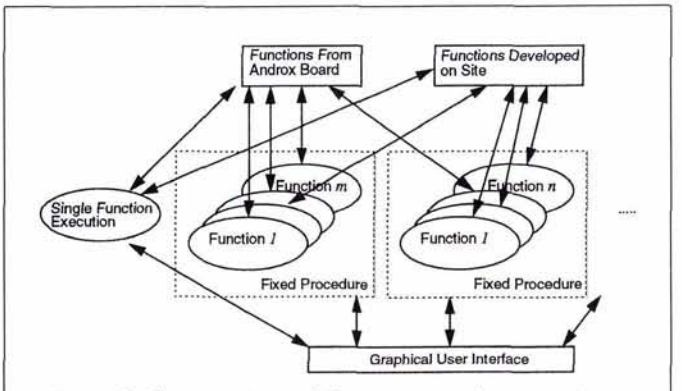

Figure 2. The structure of the STEREO software system.

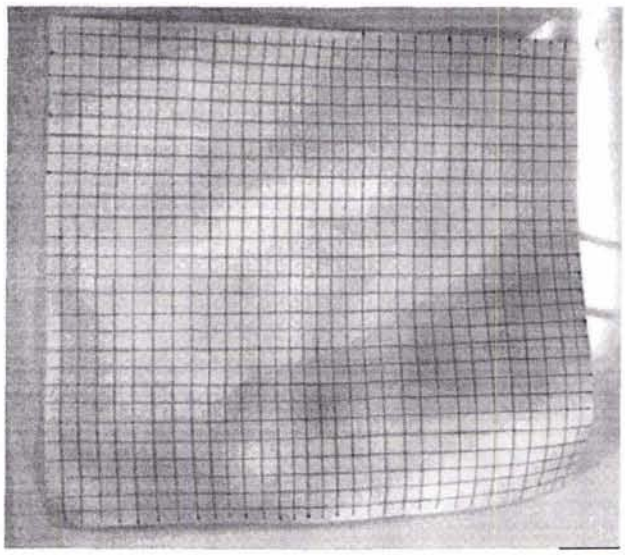

Figure 3. The averaged image of the specimen taken with the left camera.

rection). Here, the $u(t)$ is a Heaviside step function (Richards, 1986) defined by

$$u(t - t_0) = 1 \qquad \text{for } t \geq t_0$$
$$u(t - t_0) = 0 \qquad \text{for } t < t_0$$

An LMC has several attractive characteristics. It is very effective for detecting features with pixel-size width or for detecting the edge of wider features after taking the first-order derivative of the original image (Zhou, 1994). It is computationally efficient compared with frequency-domain edge-detection methods using high-pass filters after Fourier transformation. In the space domain, unlike other convolution methods using ordinary edge-detection templates (Richards, 1986), an LMC does not need to be followed by a case-specific thresholding operation to separate the highlighted features from the background. On the other hand, LMC has some shortcomings, such as its vulnerability to noise and the fact that it is directional.

Figure 3 shows an image of a specimen with a grid. Lines are detected by applying LMC with 1 by 5 templates to the reversed image, and the sub-pixel positions of the detected lines are determined with the zero-crossing method, which was first proposed by Marr and Hildreth (1980). Figure 4 shows the result of these operations. In Figure 4, if a vertical line is found to be at column s in a certain row (here s is a real number), then the pixel at column s_1 is assigned the value

$$t_1 = \lfloor (1 - s + s_1) \times 255 + 0.5 \rfloor \qquad \text{(d)}$$

and the pixel at column $s_1 + 1$ is assigned the value

$$t_2 = 255 - t_1$$

Here,

$$s_1 = \lfloor s \rfloor$$

is defined as the greatest integer smaller than s and it is assumed that pixel values are represented by 8-bit integers. The sub-pixel position of the horizontal lines are displayed in a similar way.

After extracting the grids from a stereo image pair, corresponding crosses are matched according to the geometric structure of the grids. Experiments show that the grids can be matched automatically by STEREO when the images are of ideal quality. The requirements for ideal images include that the whole grid is within the images, that no extraneous line-features other than the lines of the grid are present in the images, and that the contrast between the grid and the background is adequate. If these conditions are not met, a single pair of corresponding crosses has to be pointed out by the operator so that all other crosses in the grids can be matched automatically.

Coordinate Calculation

After feature extraction and image matching, the photogrammetric solution is accomplished using the well-known collinearity equations (Slama *et al.*, 1980). Suppose an object is located in an image taken by a CCD camera at column number C_i and row number R_i (column numbers counted from left to right in an image and row numbers from top to bottom). The image coordinates x_{ij} and y_{ij} can be found using the following relations involving C_i, R_i, and the dimensions of the CCD chip with the assumption that the principal point of the camera is at the physical center of the chip: i.e.,

$$x_{ij} = S_L \left(C_i - \frac{N_L}{2}\right) \qquad (3)$$

$$y_{ij} = S_W \left(\frac{N_W}{2} - R_i\right) \qquad (4)$$

In these two equations, N_W, N_L, S_W, and S_L are defined as in Equations 1 and 2. However, experiments showed that the actual dimensions of the CCD chips are not exactly the values as specified in the camera's manual (see the experiment section for further explanation). As a result, two coefficients K_x and K_y are introduced to make an adjustment in the CCD chip's dimensions, and Equations 3 and 4 become

$$x_{ij} = S_L K_x \left(C_i - \frac{N_L}{2}\right) \qquad (5)$$

$$y_{ij} = S_W K_y \left(\frac{N_W}{2} - R_i\right) \qquad (6)$$

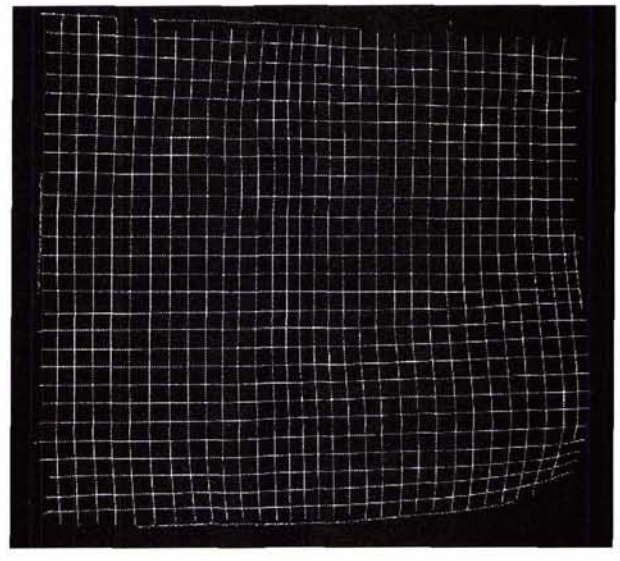

Figure 4. The grid in the image in Figure 3 extracted as zero-crossing lines.

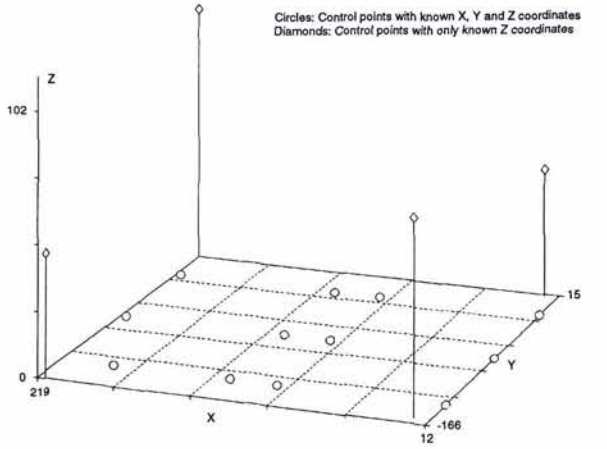

Figure 5. The distribution of the control points on the reference model (units are mm).

Substituting Equations 1, 2, 5, and 6 into the collinearity equations gives

$$\frac{LK_x}{N_L}(C_i - \frac{N_L}{2}) - x_{pp} + f\left[\frac{m_{11}(X_j - X_{ic}) + m_{12}(Y_j - Y_{ic}) + m_{13}(Z_j - Z_{ic})}{m_{31}(X_j - X_{ic}) + m_{32}(Y_j - Y_{ic}) + m_{33}(Z_j - Z_{ic})}\right] = 0 \quad (7)$$

$$\frac{WK_y}{N_W}(\frac{N_W}{2} - R_i) - y_{pp} + f\left[\frac{m_{21}(X_j - X_{ic}) + m_{22}(Y_j - Y_{ic}) + m_{23}(Z_j - Z_{ic})}{m_{31}(X_j - X_{ic}) + m_{32}(Y_j - Y_{ic}) + m_{33}(Z_j - Z_{ic})}\right] = 0 \quad (8)$$

where

The m's are elements of the rotation matrix involving the camera orientation angles ω, ϕ, and κ;
X_{ic}, Y_{ic}, and Z_{ic} provide the camera's position in object space;
X_j, Y_j, and Z_j are the coordinates of point j in the object coordinate system;
f is the focal length of the camera; and x_{pp} and y_{pp} give the position of the principal point of the camera.

As described in the *Manual of Photogrammetry* (Slama *et al.*, 1980), these two modified collinearity equations are linearized by Newton's first-order approximation, and then a least-squares solution is obtained by solving a redundant equation set iteratively. When using a traditional metric camera, only nine variables in the above equations are considered unknowns: ω, ϕ, κ, X_{ic}, Y_{ic}, Z_{ic}, X_j, Y_j, and Z_j. In STEREO, because of the unknown interior orientations of the CCD cameras, the five interior orientation parameters f, x_{pp}, y_{pp}, K_x, and K_y are also unknown. The algorithms described in the *Manual of Photogrammetry* are modified correspondingly to accommodate the new unknown variables. Among the 14 unknown parameters, some, such as f, K_x, and K_y, are correlated. As a result, initial values and weights have to be set carefully for the parameters before starting the solution. For example, very high weights have to be set for the initial unity values of K_x and K_y to guarantee the convergence of the procedure.

Experiment and Results

An 8.5- by 11-inch sheet of commercial photocopy paper was the specimen used for the experiment. A grid with 26 lines in the length direction and 31 lines in the width direction defined 806 points of interest on the surface of the specimen. The grid was drawn on the specimen with an ordinary pen and a ruler. It didn't have to be regular and served only to enhance the texture on the surface. The specimen was then humidified to cause surface deformation. The field of view was slightly larger than 8.5 by 11 inches, making the pixel size approximately

$$\frac{8.5 \times 25.4}{482} = 0.448\ (mm) \quad (9)$$

in the width direction of the specimen and

$$\frac{11 \times 25.4}{560} = 0.499\ (mm) \quad (10)$$

in the length direction of the specimen.

A well defined reference model was used to calibrate and assess the system. The model consisted of a gridded glass plate that defined object X and Y dimensions and four metal gauge blocks that provided object Z dimensions with cross-shaped markers. The positions of some of the crosses on the glass plate were measured to a precision of 0.001 mm using a comparator. The dimensions of the metal blocks were known with a precision of 0.00127 mm (0.00005 inch as specified by the manual). Twelve crosses in the grid and four points on the metal blocks were selected as control points to calibrate the system. Twenty-five points in the grid and three points on the model were selected as check points which were used to assess the results of the experiment. Figures 5 and 6 show the spatial distribution of the control points and the check points, respectively.

The experiment was conducted using the fixed procedures of STEREO. First, the two CCD cameras were set up appropriately and each of them was used to take a sequence of three images of the model. Then, without disturbing the camera setup, a sequence of three images was taken of the specimen with each camera. To lessen the effect of electrical instability in the cameras, the two sequences of the reference model images and the two sequences of the specimen images were averaged (within each sequence) to produce four images. Figures 3 and 7 show the averaged images of the specimen from the left and right camera, respectively.

When all the images were ready, the system continued with image processing/matching. During this step, the system automatically detected and determined the positions of the crosses on the reference model. Then the operator was prompted by the system to identify the points with known positions, assign them as control or check points, and enter

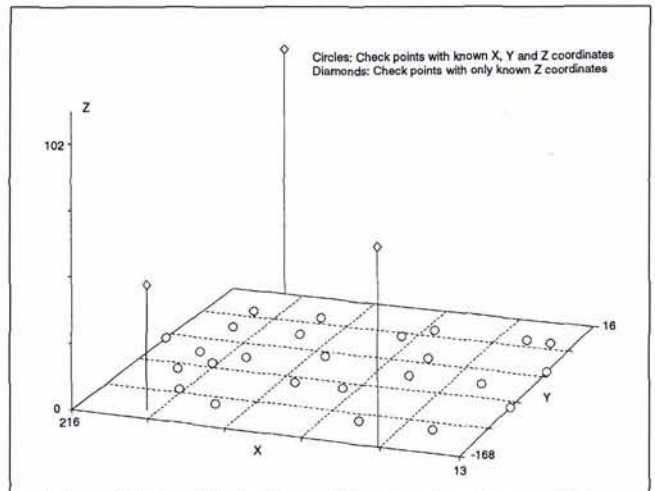

Figure 6. The distribution of the check points on the reference model (units are mm).

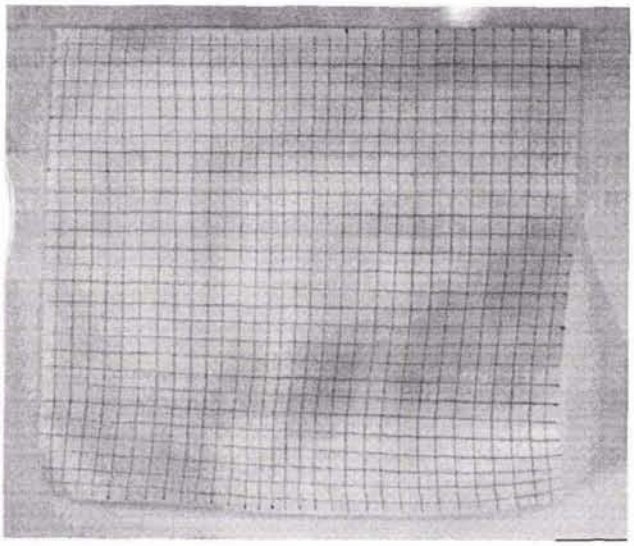

Figure 7. The averaged image of the specimen taken with the right camera.

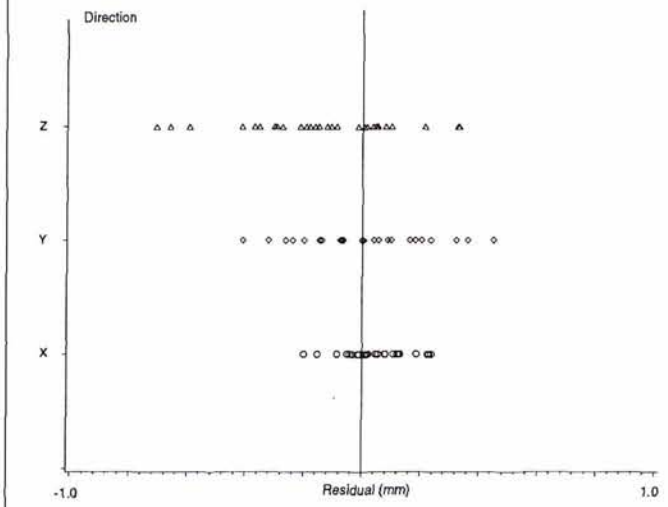

Figure 9. The distribution of the residuals around 0.0 for the check points.

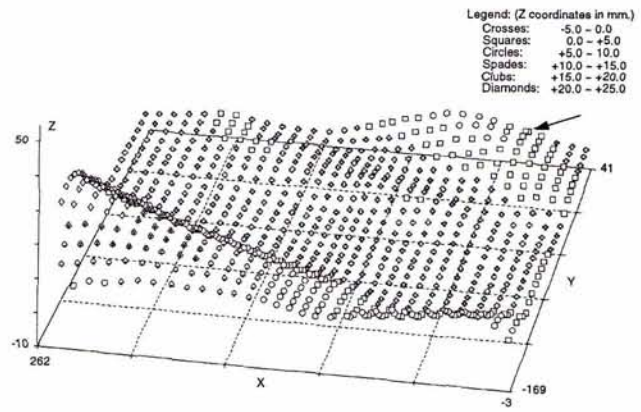

Figure 8. The distribution of the 802 points on the surface of the specimen as detected and computed by STEREO (units are mm). The arrow points to the only point that is not defined by the gird but detected by STEREO as a point of interest.

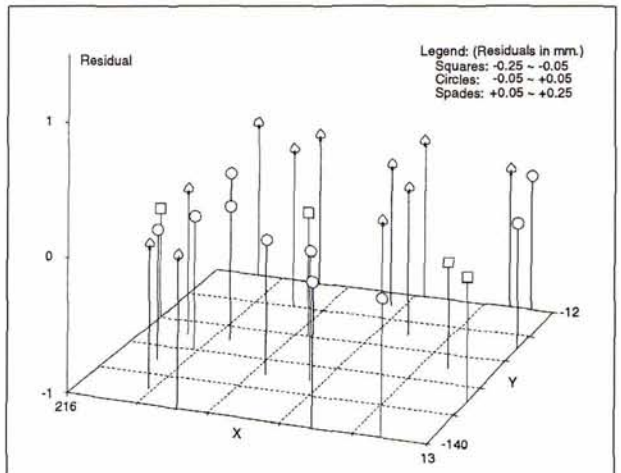

Figure 10. The residuals in X at each check point in the X-Y plane (units are mm).

TABLE 1. THE LEAST-SQUARES SOLUTION FOR THE CAMERA PARAMETERS

	Left Camera	Right Camera
ω (degree)	0.884	−0.815
ϕ (degree)	−16.399	15.178
κ (degree)	−0.051	0.949
X_{lc} (mm)	−148.851	385.159
Y_{lc} (mm)	−81.860	−59.082
Z_{lc} (mm)	921.304	906.624
x_{pp} (mm)	−0.102	0.040
y_{pp} (mm)	0.056	−0.085
f (mm)	26.572	25.999
K_x	1.004	1.004
K_y	0.994	0.994

their coordinates in the object coordinate system. In this case, the images of the specimen were good enough to be matched automatically. During coordinate calculation, the least-squares adjustment procedure solved 7015 equations for 3019 unknowns. The way to calculate the number of equations and unknowns can be found in the *Manual of Photogrammetry* (Slama *et al.*, 1980). (One hundred fifty-three extra crosses on the model whose positions were unknown were detected by the system. They were neither control points nor check points, but they participated in the least-squares solution with zero-weight initials.) The adjustment produced the following information:

- the solution for the interior and exterior orientation parameters of the cameras, as shown in Table 1;
- the X, Y, and Z coordinates of the control points and the check points, which are compared with the known values to assess the results, as indirectly shown in Figures 9, 10, 11, and 12, and Tables 2 and 3;
- the X, Y, and Z coordinates of the points of interest on the surface of the specimen, as shown in Figure 8; and

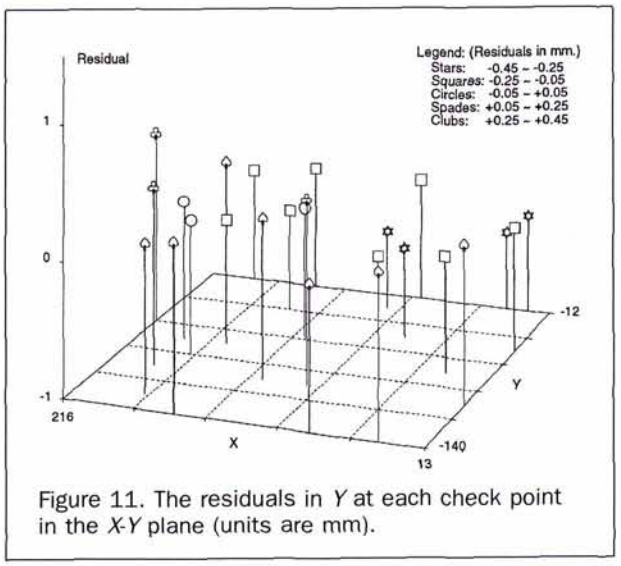

Figure 11. The residuals in *Y* at each check point in the *X*-*Y* plane (units are mm).

- the standard deviations for all values in the above three groups, as partly shown in Table 4.

Table 2 presents the statistics about the residuals (the known coordinates minus the calculated coordinates) at the control points. Table 3 contains the statistics about the residuals at the check points. Figure 9 shows graphically how the residuals at the check points are distributed around 0.0 in the *X*, *Y*, and *Z* directions. Figures 10, 11, and 12 visualize the spatial distribution of the residuals in the *X*, *Y*, and *Z* directions, respectively. In these figures, the *X* and *Y* coordinates show the distribution of the check points when they are projected onto the *X*-*Y* plane. The *Z* coordinate represents the magnitude of the residual corresponding to each check point. These figures are helpful in recognizing the distribution pattern of the residuals. The coefficients K_x and K_y were added to the least-squares adjustment procedure when it was noticed that there existed obvious patterns in the distribution of the residuals in both the *X* and *Y* directions. Before K_x and K_y were used, the *X* residuals went from negative values to positive values as *X* increased. For the increasing *Y* direction, the opposite trend occurred when positive *Y* residuals changed to negative residuals. As shown in Table 1, the solutions for K_x and K_y correspond to these trends because K_x is greater then 1.0 and K_y is smaller than 1.0.

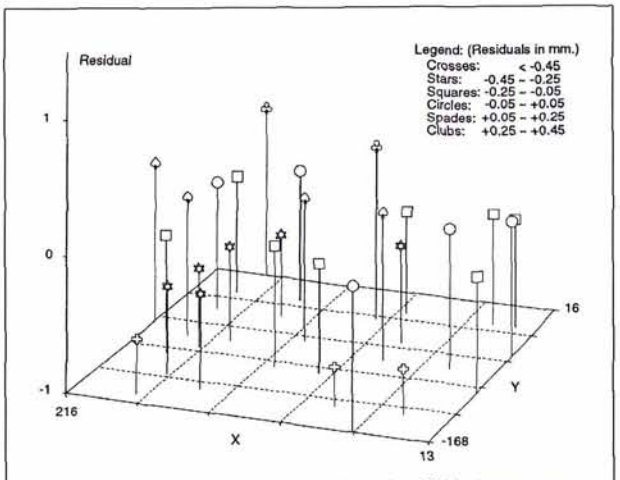

Figure 12. The residuals in *Z* at the *X*-*Y* plane projections of the check points (units are mm). There are three check points above the *X*-*Y* plane (see Figure 6).

TABLE 2. THE STATISTICS ABOUT THE RESIDUALS AT THE CONTROL POINTS (UNITS ARE MM). # OF OBS: NUMBER OF OBSERVATIONS; MIN: MINIMUM VALUE; MAX: MAXIMUM VALUE; MEAN (ABS): ARITHMETIC MEAN OF (THE ABSOLUTE) VALUES; STD: STANDARD DEVIATION OF VALUES

Direction	# of Obs	Min	Max	Mean	STD	Mean (abs)
X	12	−0.000328	0.000265	8.33E−8	0.000153	0.000108
Y	12	−0.000339	0.000332	2.26E−21	0.000198	0.000152
Z	16	−0.000066	0.000074	6.25E−8	0.000032	0.000023

TABLE 3. THE STATISTICS ABOUT THE RESIDUALS AT THE CHECK POINTS (SEE TABLE 2 FOR ABBREVIATIONS; UNITS ARE MM)

Direction	# of Obs	Min	Max	Mean	STD	Mean (abs)
X	25	−0.199	0.237	0.045	0.112	0.093
Y	25	−0.411	0.448	−0.009	0.231	0.185
Z	28	−0.709	0.331	−0.144	0.265	0.229

TABLE 4. THE STATISTICS ABOUT THE STANDARD DEVIATIONS OF THE POINTS OF INTEREST AS CALCULATED BY THE LEAST-SQUARES ADJUSTMENT (SEE TABLE 2 FOR ABBREVIATIONS; UNITS ARE MM).

Direction	# of Obs	Min	Max	Mean	STD
X	802	0.094	0.135	0.104	0.009
Y	802	0.090	0.126	0.100	0.007
Z	802	0.319	0.385	0.335	0.012

Out of the 806 points of interest defined on the surface of the specimen with the crosses of the grid, 801 were detected and their positions were computed by STEREO. One point defined by the intersection of a vertical line of the grid and the edge of the paper (pointed to by an arrow in Figure 8) was also recognized by STEREO as a point of interest. As a result, the total number of computed points was 802. In order to reconstruct a smooth surface of the specimen, a dense, well-defined regular grid consisting of 90 by 72 lines (6480 cross points) was defined just large enough to cover the 802 computed points in the *X*-*Y* plane. The *Z* coordinates of the 6480 points were calculated using bilinear interpolation based on the 802 computed points. Figure 13 shows a wireframe reconstruction of the specimen surface based on the 6480 interpolated points. Note that the *Z* coordinates are un-

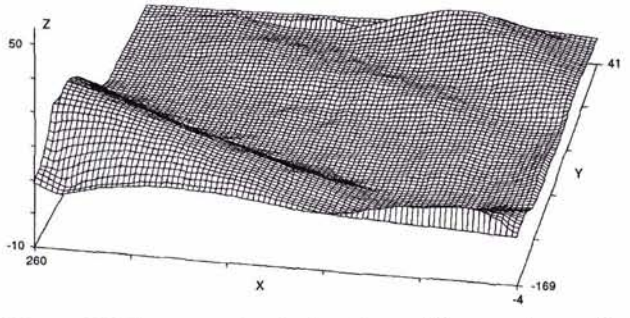

Figure 13. The reconstructed surface of the specimen after interpolation (units are mm).

reliable in some areas on the edge of the specimen where the interpolations were done with no known values in the immediate neighborhood.

Discussion

For this experiment, the mean standard deviations of the coordinates of the 802 points of interest on the surface of the specimen in the X, Y, and Z direction as calculated by the least-squares adjustment are approximately 0.104 mm, 0.100 mm, and 0.335 mm, respectively (Table 4). The solution shows better consistency in the X and Y directions than in the Z direction.

The solution fits well at the control points because their object coordinates were assigned with high weights for the least-squares adjustment (Table 2). Also as expected, the solution does not fit as well at the check points, especially in the Y and Z directions, because their object coordinates were assigned with zero weights. The average absolute residual between the known coordinate and computed coordinate at the check points is, approximately, 0.093 mm in the X direction, 0.185 mm in the Y direction, and 0.229 mm in the Z direction (Table 3), equivalent to about 19 percent, 36 percent, and 49 percent of the pixel size as calculated in Equations 9 and 10. The standard deviations of the residuals in the X, Y and Z directions are approximately 0.112 mm, 0.231 mm, and 0.265 mm, respectively. These values correspond to about 24 percent, 49 percent, and 56 percent of the pixel size. The accuracy and precision in the Y direction are much lower than that in the X direction.

Generally speaking, the residuals in the entire space of observation, if known, can be expressed by functions of the object coordinates: $R_x(X_j, Y_j, Z_j)$, $R_y(X_j, Y_j, Z_j)$, and $R_z(X_j, Y_j, Z_j)$ for residuals in the X, Y, and Z directions, respectively. The quality of a solution, if assessed by check points, depends on two factors. The first factor is the solution itself, i.e., the integration of R_x, R_y, and R_z in the entire space. With the selected set of check points, Figure 10 shows that the values of R_x are almost evenly distributed over the area spanned by the check points in the X-Y plane, with more positive ones on the upper side. Figure 11 indicates that the values of R_y are not well-balanced over the check-point area in the X-Y plane, and the best-fit zone seems to lie biased in the left hand part. There is a not-so-obvious trend in the distribution of the residuals: most of the positive residuals are in the left part of the area while most negative residuals are in the right part of the area. This phenomenon suggests that, if lower weights had been assigned to K_y at the beginning of the least-squares adjustment procedure, then the solution for K_y may have been slightly smaller than its current value listed in Table 1 and thus the residuals may have been smaller. Figures 9 and 12 both show that most values of R_z are on the negative side and are poorly balanced at the check points which are both in and above the X-Y plane. The second factor that affects the statistics about the residuals at the check points is the distribution of the check points relative to that of the control points, i.e., how R_x, R_y, and R_z are sampled. The proportion of reference points (both control and check points) with nonzero Z coordinates relative to the total number of reference points was substantially different for the control points as compared with the check points. Among the 28 check points, 25 were in the X-Y plane while, out of the 16 control points, 12 were in the X-Y plane. Also, the reference points with nonzero Z coordinates were very poorly known in the X and Y directions. If more check points occurred above the X-Y plane or the reference points with nonzero Z coordinates were well known in the X and Y directions, the statistics about the residuals might be different. In addition, if the system can be checked with more and better-distributed points in the entire three-dimensional space of observation, i.e., R_x, R_y, and R_z are better known, figures like the ones shown in Figures 10, 11, and 12 may be more representative and informative. They may help interpret the results of experiments done with the same equipment setup. For example, in this experiment, though the number of the check points is not large, the trend of residual distributions shown in Figure 11 may suggest that the Y coordinates of the points in the left hand part of Figure 8 are smaller than what they should be (remember residuals are subtractions of the computed coordinates from the known coordinates). Figure 12 may suggest that the computed Z coordinates of the points close to the X-Y plane in the lower part of Figure 8 are larger than what they should be. Recall that this paper discusses only one experiment using STEREO. These results have demonstrated some aspects of the system, but more experiments are needed to make a more comprehensive assessment.

The precision and accuracy of STEREO are acceptable relative to the resolution of the CCD cameras. The system can satisfy the needs of many mechanical deformation experiments. A few factors, such as lens distortion, image distortion due to the impact of temperature change on the CCD cameras, and sampling effects, have not been considered during the development of the system and thus may have affected the performance of the system.

The speed of the system is limited mainly by three factors: (1) the time required for human intervention; (2) the software-implemented image processing routines developed on site are very slow compared with the functions available from the Androx system; and (3) the least-squares adjustment computation takes about one minute for each iteration, depending on the number of points of interest defined on the surface. The number of iterations varies with input data and the conditions set for convergence. (It took seven iterations to produce the results reported in this paper.) For an experienced operator, 50 minutes is sufficient time to go through the procedure and produce three-dimensional coordinates for the points of interest. The step of interpolation and visual presentation requires extra time, including data transmission to other platforms. In addition, the number of points in this experiment is not the greatest that STEREO can handle. Other informal experiments processed as many as 1600 points with a single session. The exact upper limit is still unknown.

For this project, the system's degree of automation is assessed qualitatively with two criteria: (1) the degree of operator intervention and (2) the amount of special knowledge required in related fields, such as image processing, photogrammetry, and UNIX. The fixed procedures greatly increase the degree of automation of the system. With the help of step-by-step instructions, a mechanics scientist, who is not familiar with the related fields mentioned above, can operate STEREO through the entire procedure with very limited human intervention. The image matching can be accomplished automatically for images with qualities similar to the ones used in this experiment. The main inconvenience with using the system is the human input required to provide the ground coordinates of the control points. This problem can be solved by designing a reference model such that control points can be recognized automatically. The process of putting a grid onto the surface of the specimen can not be avoided because texture, in whatever form, is absolutely necessary.

Conclusion

With little human intervention, the digital system STEREO can be used to speedily determine the positions of points of interest defined with an artificial grid on a smooth surface. The computed positions exhibit a high degree of accuracy and precision relative to the pixel size of the experiment

setup. Little knowledge about image processing, photogrammetry, and computers is required of an operator.

Acknowledgments

This project is sponsored by the Empire State Paper Research Institute at the State University of New York, College of Environmental Science and Forestry. Overall support was provided by Mr. James Thorpe of the Institute. This paper has been improved based on helpful comments from the reviewers of *PE&RS*.

References

Choi, D., J. Thorpe, and R. Hanna, 1991. Image Analysis to Measure Strain in Wood and Paper, *Wood Science and Technology,* 25: 251–262.

Dowman, I. J., H. Ebner, and C. Heipke, 1992. Overview of European Developments in Digital Photogrammetric Workstations, *Photogrammetric Engineering & Remote Sensing,* 58(1):51–56.

Grimson, W. E. L., 1981. *From Images to Surfaces,* MIT Press, Cambridge, Massachusetts, 274 p.

———1985. Computational Experiments with a Feature Based Stereo Algorithm, *IEEE Transactions on Pattern Analysis and Machine Intelligence,* 7(1):17–34.

Keating, T. J., P. R. Wolf, and F. L. Scarpace, 1975. An Improved Method of Digital Image Correlation, *Photogrammetric Engineering & Remote Sensing,* 41(8):993–1002.

Marr, D., and E. Hildreth, 1980. Theory of Edge Detection, *Proceedings of Royal Society London,* 207(B):187–217.

Mason, S. O., and K. W. Wong, 1992. Image Alignment by Line Triples, *Photogrammetric Engineering & Remote Sensing,* 58(9): 1329–1334.

Richards, John A., 1986. *Remote Sensing Digital Image Analysis – An Introduction,* Springer-Verlag, Berlin, 281 p.

Schenk, T., J. Li, and C. Toth, 1991. Towards an Autonomous System for Orienting Digital Stereopairs, *Photogrammetric Engineering & Remote Sensing,* 57(8):1057–1064.

Schenk, T., and C. K. Toth, 1992. Conceptual Issues of Softcopy Photogrammetric Workstations, *Photogrammetric Engineering & Remote Sensing,* 58(1):101–110.

Slama, C. C (editor), 1980. *Manual of Photogrammetry,* 4th ed, American Society of Photogrammetry, 1056 p.

Wong, K. W., 1992. Machine Vision, Robot Vision, Computer Vision, and Close–Range Photogrammetry, *Photogrammetric Engineering & Remote Sensing,* 58(8):1197–1198.

Wong, K. W., and W. Ho, 1986. Close-Range Mapping with a Solid State Camera, *Photogrammetric Engineering & Remote Sensing,* 52(1):67–74.

Zhou, Weiyang, 1994, *A Digital System for Surface Reconstruction,* Ph.D. Thesis, the State University of New York, College of Environmental Science and Forestry.

Zhou, W., R. Brock, J. Thorpe, and P. Hopkins, 1992. A Digital Photogrammetric System for Three-Dimensional Deformation Measurement, *International Archives of Photogrammetry and Remote Sensing,* 29(B):494–500.

CALL FOR PAPERS

The American Society for Photogrammetry and Remote Sensing

announces

16TH BIENNIAL WORKSHOP ON COLOR PHOTOGRAPHY AND VIDEOGRAPHY IN RESOURCE ASSESSMENT

WESLACO, TEXAS • April 29-May 1, 1997

This workshop, following in the tradition of the pre-vious workshops, will provide an opportunity to share information on and experience with application of photo-graphic and videographic remote sensing for assessing natural resources. Emphasis will be toward, but is not limited to, the following areas:

- Plant Science
- Agricultural Crops
- Range Management
- Forest Resources
- Soils
- Video and Digital Systems
- Water Quality
- Wetlands or Riparian Vegetation
- Geomorphology
- Fisheries/Wildlife Habitat

Abstracts (250 words or less) are due by 15 January 1997.

Send abstracts to:
James H. Everitt
USDA, ARS
Remote Sensing Research Unit
2413 E. Highway 83
Weslaco, TX 78596-8344
Tel: 210-969-4824; FAX: 210-969-4893
e-mail: j-everitt@tamu.edu

Acceptance letters will be mailed by 15 February 1997.
Proceedings Papers are due 1 May 1997.